Automated Solid-Phase DNA Synthesis and Photophysical Properties of Oligonucleotides Labeled at the 5′-Terminus with $Ru(bpy)_3^{2+}$

Shoeb I. Khan, Amy E. Beilstein, Milan Sykora,† Gregory D. Smith, Xi Hu, and Mark W. Grinstaff*

Department of Chemistry, Paul M. Gross Chemical Laboratory, Duke University, Durham, North Carolina 27708

Received February 12, 1999

A facile procedure for the incorporation of $Ru(bpy)_3^{2+}$ in an oligonucleotide is reported. A $Ru(bpy)_3^{2+}$ phosphoramidite is synthesized, and then attached to the 5′-terminus of DNA using a standard protocol on an automated DNA solid-phase synthesizer. Photophysical studies of the Ru(II) tris-diimine complex as well as the corresponding labeled oligonucleotides demonstrate that the excited-state electron is localized on one specific bipyridine with the dipole directed toward the linkage to DNA, and that the Ru(II) excited state is long-lived when attached to the DNA.

Transition or lanthanide metal complexes attached to oligonucleotides at site-specific locations are of general interest for DNA/RNA sequencing, hybridization assays, anticancer treatment, and DNA-mediated energy- and electron-transfer studies.[1−8] The two main synthetic strategies toward these metallo-oligonucleotides are postmodification of the synthesized nucleic acid single strand and incorporation of a derivatized phosphoramidite for solid-phase coupling. This first strategy typically links a metal complex to the terminus of the nucleic acid single strand previously modified to contain an alkyl amine.[8−15] The second strategy, metal-derivatized phosphoramidites, exploits the use of DNA solid-phase synthetic methodologies for the site-specific labeling of an oligonucleotide with a transition metal complex. A number of groups are currently exploring this second approach,[16−22] and we have recently reported the automated solid-phase synthesis of oligonucleotides labeled with metal complexes at the nucleobase.[23−25] Herein, we report a facile and automated solid-phase procedure for the labeling of oligonucleotides at the terminus with a substitutionally inert transition metal complex, such as $Ru(bpy)_3^{2+}$. The photophysical properties of the ruthenium complex are retained after covalent attachment to DNA and unaltered by duplex formation.

Results and Discussion

$Ru(bpy)_3^{2+}$ belongs to one class of photoactive metal complexes that have been actively studied since they possess a number of favorable photochemical properties including inertness to ligand substitution reactions, tunable electronic structures, high stability, high quantum yields, and long lifetimes in fluid solution ($\tau \approx 1\ \mu s$).[26,27] The $Ru(bpy)_3^{2+}$ derivatized phosphoramidite, **4**, for automated DNA synthesis was synthesized in two steps starting from $Ru(bpy)_2Cl_2$. As shown in Scheme 1, $Ru(bpy)_2Cl_2$ was reacted with 4-methyl-2,2′-bipyridine-4′-carbonylethanolamide, **2**, in refluxing ethanol/water to yield the substitutionally inert tris-bipyridine ruthenium complex,

* Author to whom correspondence should be addressed; http://www.chem.duke.edu/∼mwg/labgroup.

† Address: University of North Carolina at Chapel Hill.

(1) Sigel, A.; Sigel, H. *Interactions of Metal Ions with Nucleotides, Nucleic Acids, and their Constituents*; Marcel Dekker Inc.: New York, 1996; Vol. 32, p 814.
(2) Sigel, A.; Sigel, H. *Probing of Nucleic Acids by Metal Ion Complexes of Small Molecules*; Marcel Dekker Inc.: New York, 1996; Vol. 33, p 678.
(3) Englisch, U.; Gauss, D. H. *Angew. Chem., Int. Ed. Engl.* **1991**, *30*, 613−629.
(4) Keller, G. H.; Manak, M. M. *DNA Probes*; Stockton Press: New York, 1993.
(5) Sammes, P. G.; Yahioglu, G. *Nat. Prod. Rep.* **1996**, 1−28.
(6) Tullius, T. D. *Metal−DNA Chemistry*; American Chemical Society: Washington, DC, 1988; Vol. 402.
(7) Clarke, M. J. *Adv. Chem. Ser.* **1997**, *253*, 349−365.
(8) Holmlin, R. E.; Dandliker, P. J.; Barton, J. K. *Angew. Chem., Int. Ed. Engl.* **1997**, *36*, 2714−2730 and references therein.
(9) Murphy, C. J.; Arkin, M. R.; Jenkins, Y.; Ghatlia, N. D.; Bossmann, S. H.; Turro, N. J.; Barton, J. K. *Science* **1993**, *262*, 1025−1029.
(10) Magda, D.; Miller, R. A.; Sessler, J. L.; Iverson, B. L. *J. Am. Chem. Soc.* **1994**, *116*, 7439−7440.
(11) Telser, J.; Cruickshank, K. A.; Schanze, K. S.; Netzel, T. L. *J. Am. Chem. Soc.* **1989**, *111*, 7221−7226.
(12) Bannwarth, W.; Schmidt, D.; Stallard, R. L.; Hornung, C.; Knorr, R.; Müller, F. *Helv. Chim. Acta* **1988**, *71*, 2085−2099.
(13) Bashkin, J. K.; Frolova, E. I.; Sampath, U. *J. Am. Chem. Soc.* **1994**, *116*, 5981−5982.
(14) Sigman, D. S. *Acc. Chem. Res.* **1986**, *19*, 180−186.
(15) Bergstrom, D. E.; Gerry, N. *J. Am. Chem. Soc.* **1994**, *116*, 12067−12068.
(16) Manchanda, R.; Dunham, S. U.; Lippard, S. J. *J. Am. Chem. Soc.* **1996**, *118*, 5144−5145.
(17) Schliepe, J.; Berghoff, U.; Lippert, B.; Cech, D. *Angew. Chem., Int. Ed. Engl.* **1996**, *35*, 646−648.
(18) Bannwarth, W.; Schmidt, D. *Tetrahedron Lett.* **1989**, *30*, 1513−1516.
(19) Meggers, E.; Kusch, D.; Giese, B. *Helv. Chim. Acta* **1997**, *80*, 640−652.
(20) Hurley, D. J.; Tor, Y. *J. Am. Chem. Soc.* **1998**, *120*, 2194−2195.
(21) Magda, D.; Crofts, S.; Lin, A.; Miles, D.; Wright, M.; Sessler, J. L. *J. Am. Chem. Soc.* **1997**, *119*, 2293−2294.
(22) Lewis, F. D.; Helvoigt, S. A.; Letsinger, R. L. *Chem. Commun.* **1999**, 327−328.
(23) Khan, S. I.; Beilstein, A. E.; Grinstaff, M. W. *Inorg. Chem.* **1999**, *38*, 418−419.
(24) Khan, S. I.; Beilstein, A. E.; Smith, G. D.; Sykora, M.; Grinstaff, M. W. *Inorg. Chem.* **1999**, *38*, 2411−2415.
(25) Khan, S. I.; Grinstaff, M. W. *J. Am. Chem. Soc.* **1999**, *121*, 4704−4705.
(26) Damrauer, N. H.; Cerullo, G.; Yeh, A.; Boussie, T. R.; Shank, C. V.; McCusker, J. M. *Science* **1997**, *275*, 54−57.
(27) Balzani, V.; Juris, A.; Venturi, M.; Campagne, S.; Serroni, S. *Chem. Rev.* **1996**, *96*, 759−833.

10.1021/ic990177y CCC: $18.00
Published on Web 08/05/1999

Scheme 1

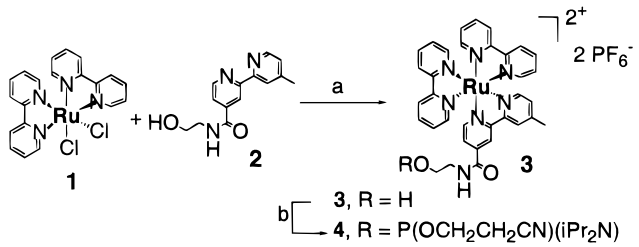

(a) 70% EtOH/H_2O, 82% yield ; (b) $ClP(OCH_2CH_2CN)(iPr_2N)$, DIPEA, CH_3CN, 78% yield.

Scheme 2

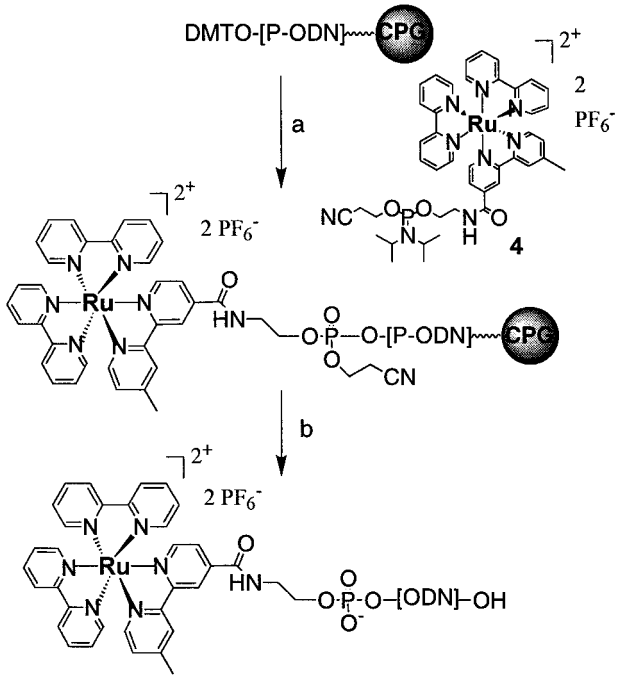

5 5'-**Ru**-TCA ACA GTT TGT AGC A-3'
6 5'-**Ru**-ATAAATAT-3'
7 5'-**Ru**-ATAAGTAT-3'
8 5'-**Ru**-TGC TAC AAA CTG TTG A-3'
9 5'-TCA ACA GTT TGT AGC A -3'
10 5'-TGC TAC AAA CTG TTG A-3'

(a) normal synthesis, ruthenium phosphoramidite coupling; (b) 30% NH_3, 55 °C, 16 h. ODN = oligodeoxynucleotide; P-ODN = protected oligodeoxynucleotide

3. This complex was isolated as the PF_6^- salt, which ensured sufficient solubility in organic solvents for subsequent use in an automated DNA synthesizer. Next, 2-cyanoethylchloro-*N*,*N*-diisopropylphosphoramidite was reacted with **3** in dry CH_3CN to afford the metallo-phosphoramidite, **4**. The ruthenium-phosphoramidite was added to the 5′-terminus of an oligonucleotide during automated synthesis (Scheme 2).[28,29] Syntheses were performed at both the 0.2 and 1.0 μmol scales on an ABI 392 DNA synthesizer using the standard coupling protocol with the metallo-phosphoramidite introduced at the last step in the reaction sequence. Once the ruthenium-labeled oligonucleotide was synthesized, the modified oligonucleotide was cleaved from the column. The nitrogenous bases and phosphate groups were next deprotected in 30% ammonium hydroxide at 55 °C for 16 h. Finally, the metallo-oligonucleotide was purified using reverse-phase HPLC and characterized by electrospray mass spectrometry.

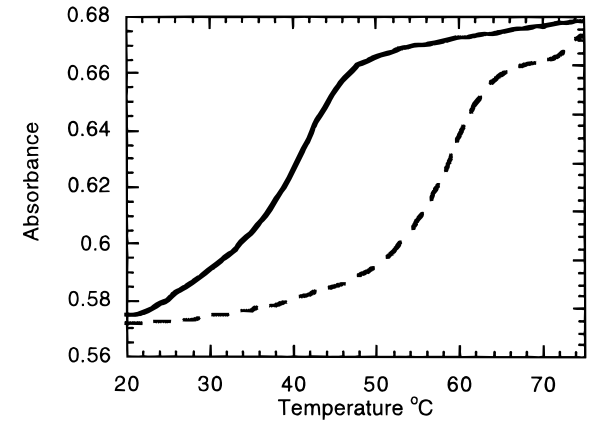

Figure 1. Melting curve for ruthenium-labeled duplex, **5·10** (solid line), and unmodified duplex, **9·10** (dashed line).

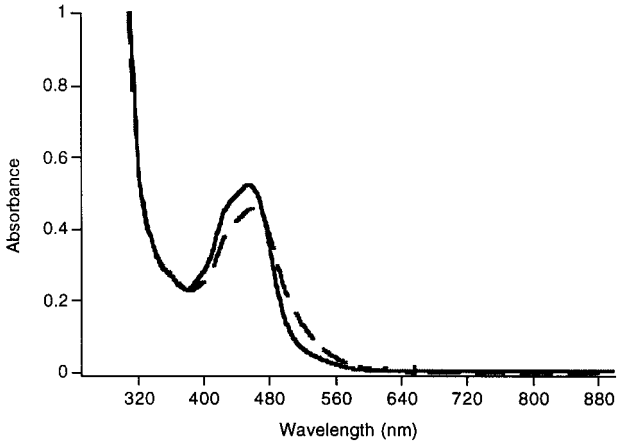

Figure 2. Electronic absorption of **3** (solid line) and **5** (dashed line) in aqueous solution at 25 °C.

The melting temperature (T_m) of the ruthenium-modified oligonucleotide duplex, **5·10**, is 42 °C compared to 60 °C for the unmodified duplex, **9·10** (5 mM sodium phosphate, 50 mM NaCl; pH = 7; monitoring at 260 nm; Figure 1). The decrease in T_m reflects the relative ease with which the two DNA strands separated, most likely as a consequence of steric crowding by the metal complex at the 5′-terminus. The $Ru(bpy)_3^{2+}$ is connected via a short ethylene spacer to the terminal phosphate, unlike previous metallo-oligonucleotides labeled at the terminus.[18] This magnitude of T_m decrease is not observed when the metal complex is connected, via a short linker, to a terminal or internal nucleobase of an oligonucleotide.[23]

The absorption spectrum of the derivatized ruthenium tris-bipyridine complex, **3**, exhibits the characteristic metal-to-ligand charge-transfer band (^1MLCT-$^1A_1$) centered at 460 nm, analogous to $Ru(bpy)_3^{2+}$ (Figure 2). Excitation of this MLCT band of **1** produces an emission centered at 670 nm slightly red-shifted relative to $Ru(bpy)_3^{2+}$. The emission lifetime of **3** in phosphate buffer is 407 ns. To further characterize the excited state of **3**, the ground- and excited-state infrared spectra were measured using step−scan Fourier transform infrared (S^2FTIR) time-resolved spectroscopy.[30−33] The ground- and excited-state infrared $\bar{\nu}$(C═O) band energies of **3** are 1672 and 1643 cm^{-1},

(28) Caruthers, M. H. *Acc. Chem. Res.* **1991**, *24*, 278−284.
(29) Gait, M. J. *Oligonucleotide Synthesis: A Practical Approach*; IRL Press: Washington, DC, 1984; p 217.

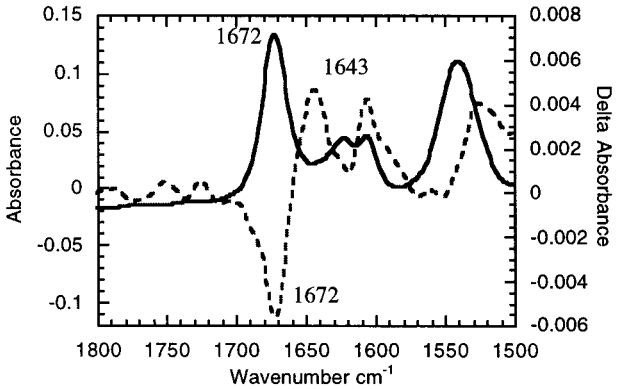

Figure 3. FT-IR ground-state (solid line) and laser-induced ΔA spectra (dashed line) in CD_3CN of **3**.

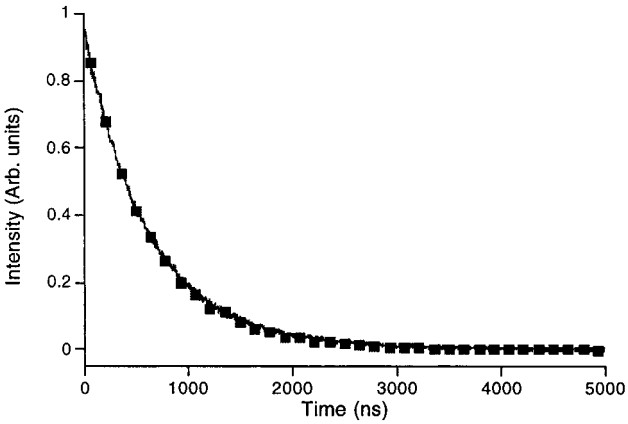

Figure 4. Emission decay trace monitored at 640 nm for ruthenium-labeled oligonucleotide, **5** (solid line), and duplex, **5·10** (blocks), after 455 nm pulse excitation.

respectively (Figure 3). This negative $\bar{\nu}$(C═O) shift of ≈29 cm^{-1} indicates that on the nanosecond time scale the excited-state electron is localized on the amide-bearing bipyridine, and that the lowest π^* acceptor level contains significant C═O character. The magnitude of this $\bar{\nu}$(C═O) shift is approximately double that observed for a diamide substituted bipyridine ($\bar{\nu} \approx 15$ cm^{-1}), further supporting the assignment of the excited-state electron to the amide-substituted pyridine ring of **3**.[33,34] Importantly, the excited-state electron is localized to one bipyridine and the excited-state dipole is oriented toward the amide tether to the oligonucleotide.

The absorption spectra of the ruthenium-labeled single strand, **5**, and duplex, **5·10**, exhibit the characteristic metal-to-ligand charge-transfer band (^{1}MLCT-$^1A_1$) centered at 465 nm, similar to **3** (Figure 2). The emission is centered at 670 nm for both the single strand, **5**, and the duplex, **5·10**. The emission lifetime in phosphate buffer (5 mM sodium phosphate, 50 mM NaCl, pH = 7; 5×10^{-6} DNA concentration) of the ruthenium-labeled oligonucleotide, **5**, is 616 ns, and that of the modified oligonucleotide duplex, **5·10**, is 629 ns (Figure 4). The ruthenium excited state is not quenched by the oligonucleotide, an observation consistent with the redox potentials of A, C, G, and T.[35]

Conclusions

In summary, the facile preparation of oligonucleotides labeled at the 5′-terminus with a coordinatively saturated metal complex is reported that utilizes automated DNA solid-phase synthesis and a $Ru(bpy)_3^{2+}$−phosphoramidite. Time-resolved step−scan Fourier transform infrared (S^2FTIR) studies of the Ru(II) tris-diimine complex show the excited-state electron to be localized on the amide-substituted bipyridine. The $Ru(diimine)_3$ complex possesses a long lifetime in fluid solution, and this property is retained after covalent attachment to the oligonucleotide. These metallo-oligonucleotides are well suited for energy- and electron-transfer studies with complementary oligonucleotides containing quenchers such as $Os(bpy)_3^{2+}$ or phenothiazine.[36]

Experimental Section

All solvents were dried and distilled prior to use. Absorption spectra were measured on a Hewlett-Packard 8452 diode array spectrometer. Emission spectra were recorded on a Perkin-Elmer LS50B or Spex Fluorolog-2 emission spectrometer. Reverse-phase HPLC was performed on a Ranin HPLC with a C18 column monitoring at 254 and/or 450 nm.

A. Syntheses. 4′-Methyl-2,2′-bipyridine-4-carboxaldehyde and 4′-methyl-2,2′-bipyridine-4-carboxylic acid were synthesized following the procedure described by Meyer and Erickson.[37]

4′-Methyl-2,2′-bipyridine-4-carboxaldehyde: yield 33%; FAB-MS calcd for $C_{12}H_{10}N_2O$ 198, found [M + H] 199; ^{1}H NMR (DMSO-d_6) δ 2.45 (s, 3H, CH_3), 7.15−8.8 (m, 6H, py); 10.1 (s, 1H, CHO).

4′-Methyl-2,2′-bipyridine-4-carboxylic acid: yield 77%; FAB-MS calcd for $C_{12}H_{10}N_2O_2$ 214, found [M + H] 215; ^{1}H NMR (DMSO-d_6) δ 2.5 (s, 3H, CH_3), 7.15−9 (m, 6H, py).

4′-Methyl-2,2′-bipyridine-4-ethanolamide, (4-m-4′ea-bpy), 2. 4′-Methyl-2,2′-bipyridine-4-carboxylic acid (0.42 g, 2 mmol) was dissolved in DMF (20 mL). HOBt (0.31 g, 2 mmol), DIPEA (0.39 mL, 2.2 mmol), and ethanolamine hydrochloride (0.22 g, 2.1 mmol) were added, and the solution was cooled in ice. DCC (0.45 g, 2.2 mmol) was dissolved in DMF (3 mL) and added dropwise to the reaction mixture. The mixture was stirred at room temperature overnight. The DCU that formed was filtered off, and the solvent was removed by vacuum distillation. The remaining solid compound was dissolved in ethyl acetate, washed with $NaHCO_3$ (5%), 0.5 N HCl, and brine, and dried over sodium sulfate. The solvent was removed by rotary evaporation, and the compound was purified by column chromatography using 5% methanol in chloroform as eluent (0.39 g; 76%). ^{1}H NMR (DMSO): δ 2.4 (s, 3H, CH_3), 3.3 (t, 2H, CH_2), 3.5 (t, 2H, CH_2), 7.2−8.8 (m, 6H, py). FAB-MS calcd for $C_{14}H_{15}N_3O_2$: $[M]^+$ 257.1. Found: $[M + H]^+$ 258.1.

Ruthenium(II)-bis(bipyridine)(4-methyl-4′-ethanolamide-bipyridine) Bis(hexafluorophosphate), 3. $Ru(bpy)_2Cl_2$ (**1**, 0.29 g, 0.6 mmol) was added to a solution of 4′-methyl-2,2′-bipyridine-4-ethanolamide, **2** (0.21 g, 0.82 mmol), in 70% ethanol/H_2O (25 mL) and refluxed for 10 h. Next, the reaction mixture was cooled and ethanol was removed in vacuo. After standing for 4 h at room temperature, the solution was filtered and the solid compound washed with cold water. A saturated aqueous solution of NH_4PF_6 was added until no further precipitate was observed. The mixture was kept at room temperature for an additional 2 h and then finally filtered, washed with cold water and ether, and dried overnight to give 0.47 g (82%) of a pure orange compound. ^{1}H

(30) Chen, P.; Omberg, K. M.; Kavalinus, D. A.; Treadway, J. A.; Palmer, R. A.; Meyer, T. J. *Inorg. Chem.* **1997**, *36*, 954−955.
(31) Schoonover, J. R.; Strouse, G. F.; Dyer, R. B.; Bates, W. D.; Chen, P.; Meyer, T. J. *Inorg. Chem.* **1996**, *35*, 273−274.
(32) Palmer, R. A.; Chao, J. L.; Dittmar, R. M.; Gregoriou, V. G.; Plunkett, S. E. *Appl. Spectrosc.* **1993**, *47*, 1297−1310.
(33) Omberg, K. M.; Smith, G. D.; Kavaliunas, D. A.; Chen, P.; Treadway, J. A.; Schoonover, J. R.; Palmer, R. A.; Meyer, T. J. *Inorg. Chem.* **1999**, *38*, 951−956.
(34) Danzer, G. D.; Golus, J. A.; Kincaid, J. R. *J. Am. Chem. Soc.* **1993**, *115*, 8643−8648.
(35) Steenken, S.; Jovanovic, S. V. *J. Am. Chem. Soc.* **1997**, *119*, 617−618.
(36) Grinstaff, M. W. Unpublished results.
(37) Peck, B. M.; Ross, G. T.; Edwards, S. W.; Meyer, G. I.; Meyer, T. J.; Erickson, B. W. *Int. J. Pept. Protein Res.* **1991**, *38*, 114−123.

NMR (DMSO): δ 2.4 (s, 3H, CH_3), 3.4 (t, 2H, CH_2), 3.8 (t, 2H, CH_2), 7.2−9.2 (m, 22H, py). UV−vis (CH_3CN): λ_{max} 454 nm. FAB-MS calcd for $C_{34}H_{31}N_7O_2RuP_2F_{12}$: $[M - 2PF_6^-]^+$ 670.3, $[M - PF_6^-]^+$ 815.2. Found: $[M - 2PF_6^-]^+$ 671.3, $[M - PF_6^-]^+$ 816.2. HR FAB-MS calcd: 671.1559. Found: 671.1535.

Phosphoramidite Synthesis.[38] Ruthenium(II)-bis(bipyridine)(4-methyl-4′-ethanolamide-bipyridine) bis(hexafluorophosphate), **3** (0.19 g, 0.2 mmol), was coevaporated in dry CH_3CN twice and finally dissolved in CH_3CN (5 mL). Next, DIPEA (0.14 mL, 0.8 mmol) was added followed by 2-cyanoethyl chloro-*N*,*N*-diisopropoyl phosphoramidite (0.067 mL, 0.3 mmol), and the mixture was stirred for 5 h. The solvent was then evaporated and the compound dissolved in CH_3CN and precipitated in dry ether to afford the ruthenium phosphoramidite, **4** (0.18 g, 78%), which was used without further purification. ^{1}H NMR ($CDCl_3$): δ 148.4 and 148.6 ppm.

Automated DNA Synthesis. The oligonucleotides were synthesized from the 3′ to 5′ end on both the 0.2 and 1.0 μmol scale using standard automated DNA synthesis (on an ABI 395 DNA synthesizer) and reagents purchased from Glen Research. A 0.1 M solution of ruthenium-(2-cyanoethyl-*N*,*N*-diisopropyl)phosphoramidite, **4**, in dry acetonitrile was prepared in a standard reagent bottle and installed on the DNA synthesizer. A standard automated solid-phase synthesis was performed, except that the reaction time for the modified phosphoramidite was increased to 900 s. After synthesis the oligonucleotide was cleaved from the solid support and incubated at 55 °C in NH_3 overnight to completely deprotect the oligonucleotide. Collection and analysis of the DMT fractions (498 nm) during automated synthesis showed efficient phosphoramidite coupling (>98%) for the A, C, G, and T phosphoramidites. The metallo-oligonucleotide was purified using reverse-phase HPLC (C18; 0.1 M TEAA/CH_3CN; 10−50% gradient over 50 min; monitoring at 254 and/or 450 nm). HPLC traces of the crude reaction mixture showed both unmodified (≈15−25%) and modified oligonucelotides (≈75−85%). The purified ruthenium-modified oligonucleotides exhibited one peak in an HPLC trace, with retention times greater than the corresponding unmodified oligonucleotide. Electrospray mass spectrometry of the metallo-oligonucleotide confirmed formation (e.g., ruthenium-modified oligonucleotide **5**, 1403: 1403.5 calcd:found for the +4 charged state; the +5 and +3 charged states were also observed).

B. Melting Curves. The stability of the duplex formed between two complementary oligonucleotides was determined by analyzing the melting curve profile. Briefly stated, 2 mM stock solutions of the separate oligonucleotides were prepared and diluted to a working solution of 0.5 absorbance units. Next the two solutions were combined, and the resulting solution was heated to 90 °C for 5 min. The solution was then allowed to cool to room temperature over 3 h. After cooling, the thermal denaturation experiment was performed using the following parameters on a AVIV Spectrophotometer model 17DS UV−vis−IR: (a) monitoring wavelength, 260 nm; (b) temperature range, 20−80 °C; (c) temperature step, 0.5 °C; (d) averaging time constant, 45 s; (e) temperature overshoot, 0.2 °C; (f) time overshoot, 1 s; (g) rate of change for the temperature step, 10 °C/min; and (h) equilibrium time, 30 s.

C. Physical Studies. Emission Spectra. Emission spectra were recorded on a Spex Fluorolog-2 emission spectrometer equipped with a 450 W Xe lamp and cooled Hammamatsu R928 photomultiplier. The recorded emission spectra were corrected for spectrometer response. The calibration curve was obtained using a NIST calibrated standard lamp (Optronics Laboratories, Inc., model 220M) controlled with a precision current source at 6.5 W (Optronics Laboratories, Inc., model 65) and by following the procedure recommended by the manufacturer. The spectra were obtained in buffer at room temperature in a 1 cm quartz cell using right angle observation of emitted light.

Lifetimes. A Laser Photonics LN1000 nitrogen laser-LN102 dye laser (coumarin 460 dye, Exciton) was used as the irradiation source. The emission was monitored at a right angle with a Macpherson 272 monochromator and Hammamatsu R666-10 PMT. The signal was processed by a LeCroy 7200A transient digitizer interfaced with an IBM-PC. The excitation wavelength was 455 nm, and the monitoring wavelength was 640 nm. Power at the sample was 120 μJ/pulse as measured by a Molectron J3-09 power meter. The measured instrument lifetime response is 10 ns (fwhm). The acquired emission decay curves were analyzed by locally written software based on the Marquardt algorithm.

S^{2}FTIR. The transient data were measured on a step−scan modified Bruker IFS88 spectrometer with a standard globar source and dry air purge. The samples were dissolved in CD_3CN to give an absorbance between 0.125 and 0.5 in a 250 mm path length cell for the amide bond analyzed. Samples were deoxygenated by sparging with argon for 60 min and were loaded into a CaF_2-window cell by syringe under argon. The ground-state IR spectrum was corrected for absorption due to trace amounts of water collected during sample handling.

The samples were excited using the third harmonic (355 nm, 10 ns, 10 Hz, 3 mJ/pulse) from a Q-switched Quanta-Ray DCR-1A Nd:YAG laser. The laser excitation and data acquisition were synchronized with a Stanford Research model DG535 pulse generator. An AC/DC-coupled photovoltaic Kolmar Technologies mercury cadmium telluride (MCT) detector with a 50 MHz preamplifier and an effective rise time of ∼20 ns was used to sample the transmitted infrared signal. The AC signal was further amplified by a Stanford Research model SR445 preamplifier (×250) before being directed to a personal computer equipped with a 100/200 MHz PAD82a transient digitizer. The DC signal was sent directly to the digitizer to be used for phase correction of the AC signal. The data were processed using Bruker Instruments' Opus 3.0 software.

To minimize data collection times, the spectral window observed was limited to 1150−2250 cm^{-1} by the CaF_2 cell windows and a germanium low-pass filter placed over the detector window. The interferogram response before and after each laser flash was digitized at 10 ns intervals, and data from 210 laser flashes were averaged at each point. Data collection time was approximately 2 h. The ΔA spectra were calculated from the single beam ΔI transforms by the relation $\Delta A(\upsilon,t) = -\log[1 + \Delta I(\upsilon,t)/I(\upsilon)]$, where $I(\upsilon)$ is the detected intensity before laser excitation and $\Delta I(\upsilon,t)$ is the change in intensity at time t. For the ΔA "snapshot," 10 postexcitation time slices were averaged for greater signal to noise.

Acknowledgment. This work was supported in part by NSF (CAREER), Petroleum Research Fund, administered by the American Chemical Society (PRF 32875-G3), PE-Applied Biosystems, and Duke University. A NSF Graduate Fellowship Program to G.D.S. is gratefully acknowledged. We thank Professors T. J. Meyer, R. A. Palmer, and M. C. Fitzgerald for instrumentation use.

IC990177Y

(38) McBride, L. J.; Caruthers, M. H. *Tetrahedron Lett.* **1983**, *24*, 245−248.